Improving the Control Performance of Jacking System of Jack-Up Rig Using Self-adaptive Fuzzy Controller Based on Particle Swarm Optimization

Tien-Dat Tran[1], Viet-Dung Do[1,2], Xuan-Kien Dang[1(✉)], and Ba-Linh Mai[3]

[1] Ho Chi Minh City University of Transport, Ho Chi Minh City, Vietnam
kien.dang@ut.edu.vn
[2] Dong An Polytechnic, Binh Duong, Vietnam
[3] Ministry of Transportation, Ha Noi, Vietnam

Abstract. Oil and gas Jack-up Rig is a type of offshore production for exploitation with complex structure and working modes, capable of operating independently at sea. Although Vietnam has rich petroleum resources, the exploitation equipment, particularly jack-up rigs, almost depends on international technologies. Therefore, the subject of an advanced control theory for the jacking system of Jack-up Rig is a critical issue. In this work, we study the Particle swarm optimization approach based on a Fuzzy controller to adapt to the effects of environmental forces and hydrodynamic amplification. The designed Fuzzy Particle Swarm Optimization controller is compared with the Fuzzy Proportional Integral Derivative controller in order to verify the advantage of the proposed method. By using Matlab software, the simulation results show the advantages of the suggested approach.

Keywords: Hydrodynamic amplification · Environmental forces · Fuzzy particle swarm optimization · Jacking system

1 Introduction

For decades, Jack-up drilling platforms have been utilized for offshore oil and gas exploration, drilling, and work-over. There are several techniques [1–4] for stable control and decreasing influencing factors in the jacking process of a Jack-up Rig (JuR). Even while each technique has its benefits, the study of advanced control algorithms continuously motivates researchers to develop theory and practice solutions to assist the system function more reliably and securely control system and has many more operations that were not possible previously.

In general, the rig move system and the jacking system are the two most significant control systems for JuR. For these two systems' outstanding advantages, many researchers are committed to creating enhanced technology and artificial intelligence [5–10]. Several suggested advanced control methods, such as Fuzzy [5], Hybrid Fuzzy

N.-S. Vo et al. (Eds.): INISCOM 2022, LNICST 444, pp. 184–200, 2022.
https://doi.org/10.1007/978-3-031-08878-0_13

[6], Fuzzy Adaptive [7], Neural Network [8], Genetic Algorithm (GA) [9], and Particle swarm optimization (PSO) [10], have shown their effectiveness and stability. In the meanwhile, several traditional controllers like the PID and the Linear Quadratic Regulator (LQR) are still in use for the jacking systems. Furthermore, there are few research on the application of current control theory to improve the quality and performance of controllers, particularly jacking systems.

Recently, the Fuzzy Control (FC) has received plenty of innovative results in achievements of literature [6, 7] to cope with problems of unpredictability and disturbance. The FC method preserves all closed-loop signals within the constraints of a class of switching signals with typical dead-time. The Adaptive Fuzzy Control (AFC) is also seen to be an effective technique for improving the control performance of the fuzzy controller [11, 12], especially for the self-adaptive fuzzy control (SAFC) [13–15]. On the other hand, optimal algorithms such as GA and PSO are being studied and applied in combination with fuzzy logic to increase the adaptability and stability of the SAFC. By the way, the controller does not only ensures the control performance but also enhances the robustness. Finally, this is the motivating factor for our choice to employ the innovative technique for JuR's jacking control system, as it must operate in harsh environmental conditions.

Related to the Rig building in Vietnam, the automatic controller does not play an important role in rig construction. Due to the fuzzy system's capacity to simulate a nonlinear composition, the hierarchical fuzzy model fits out a suitable approach for the JuR with unpredictable affects. In this study, we used the SAFC based on the PSO called Fuzzy Particle Swarm Optimization (FPSO) to improve the control performance of the Jacking system of the JuR. The following are the primary contributions of this paper: (i) We constructed the mathematical modeling of the Jacking system after performing movements of the JuR in the axis; (ii) We realize that the Fuzzy PID (FPID) controller designed for the Jacking system is not highly feasible under the influence of internal and external loads by simulation results. Therefore, our suggested controller, one kind of the SAFC, is the FPSO aiming to solve the aforementioned issue; (iii) Finally, the simulation of the designed FPSO is compared with the FPID controller in order to verify the advantage of the proposed approach.

This paper is organized as follows. The mathematical modeling of the Jacking system is presented in Sect. 2, and Sect. 3 analyzes the affected factors including internal and external load. Section 4 represents the JuR control methods. The simulation results and discussion of the three case studies are expressed in Sect. 5, followed by the concluding remarks of this study in Sect. 6.

2 Mathematical Modeling of Jacking System

2.1 The Movements of the Jack-Up Rig

The movements of the Jack-up Rig are shown in Fig. 1. The rig moves along the X direction, transversely vibrates in the Y direction, and moves up and down in the Z direction. However, vertical and horizontal shaking of the rig body oscillates around the X-axis, Y-axis while rotating around the vertical Z-axis. In lifting mode, the jacking

system is driven by electric motors mounted on the body of the truss. The motors on each axis operate synchronously and are the same type and parameters.

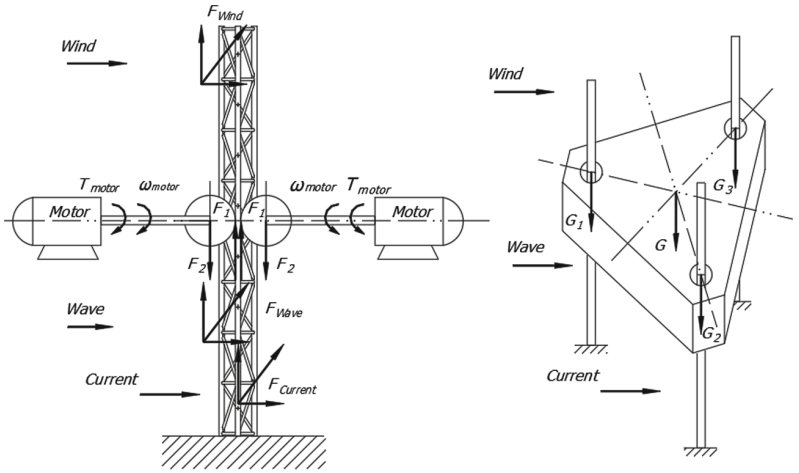

Fig. 1. Movement of the Jack-up Rig [16].

2.2 Mathematical Model of the Jacking Control System

In actual operating conditions, the sensor system determines the current displacement position of the JuR under the influence of disturbances. Based on the error between the desired position and the actual position, the controller computes the value of the control signal to transmit to the thrust allocation. Here, the thrust allocation converts the control signal into control commands (such as the direction of rotation, speed, and torque on the motor shaft) for distribution to thurster dynamics. The motors at the rig legs will operate according to the control command to carry out the process of lifting and lowering the platform. From there, the JuR's kinematic model will move, and the sensor system continues to determine the new position of the JuR. The overall diagram of the Jacking control system is shown in Fig. 2. The system of differential equations describing the JuR's kinematics is given as [17–20]

$$M\frac{d^2x(t)}{dt^2} + C\frac{dx(t)}{dt} + Kx(t) = \tau_m(t) + \tau_d(t) \tag{1}$$

where $M = \sum_{i=0}^{n} m_i$ is total weight of JuR, C and K are damping and stiffness of the single degree of freedom (SDOF) system, $\tau(t) = \tau_m(t) + \tau_d(t)$, $\tau_m(t) = \sum_{i=0}^{n} \tau_i(t)$ is the total torque on motor shafts, $x(t)$ is the displacement of the hull.

The total effect of load including wave, wind, current, and external load, respectively

$$\tau_d(t) = \tau_{wave}(t) + \tau_{wind}(t) + \tau_{current}(t) + \tau_1(t) \tag{2}$$

The displacement of the hull is calculated by

$$x(t) = R\theta(t) \tag{3}$$

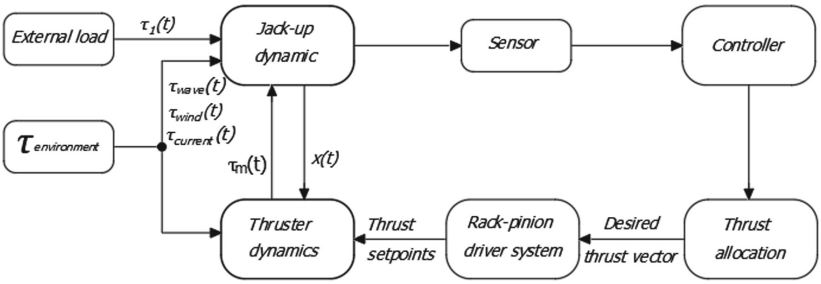

Fig. 2. An overall diagram of the Jacking control system.

therein, R expresses the effective radius of the pinion, and $\theta(t)$ is the angular of the pinion. From the Eqs. (1) and (3), the JuR's hull kinematics is written as

$$Rs^2\theta(s)\sum_{i=1}^{n} m_i + RCs\theta(s) + KR\theta(s) = \tau(s) \tag{4}$$

The transfer function of the JuR kinematics model (the Jack-up dynamic block expresses in Fig. 2) is given as

$$G_{JuR} = \frac{\theta(s)}{\tau(s)} = \frac{k_e}{Ms^2 + Cs + K} \tag{5}$$

with $k_e = 1/R$ is the conversion factor in rotary translational transmission (including the number of motors and transmission coefficient). The rig body is raised through the rack and pinion systems. By using DC motors, the thruster dynamics provide torque for the drivetrain. The driving DC motor torque is calculated as [21]

$$\begin{aligned} L_a\dot{I}_a + R_aI_a + K_bW_m &= V \\ \tau_m &= K_tI_a \end{aligned} \tag{6}$$

where K_t is torque constant, K_b is back emf constant, V is input voltage, I_a is armature current, R_a is armature resistance, J is rotor inertia, D_a is viscous friction constant, W_m is angular velocity and L_a is inductance. Therefore, the transfer function of the thruster dynamics is performed as

$$G_{Th} = \frac{W(s)}{V(s)} = \frac{k_t}{JL_as^2 + (R_aJ + L_aD_a)s + (R_aD_a + K_bK_t)} \tag{7}$$

The jacking system consists of a jack-up dynamic and thruster dynamic (shown in Fig. 2). From the Eqs. (5) and (7), the transfer function of the jacking system is determined as

$$G = G_{JuR}.G_{Th} = \frac{k_e}{Ms^2 + Cs + K}\frac{k_t}{JL_as^2 + (R_aJ + L_aD_a)s + (R_aD_a + K_bK_t)} \tag{8}$$

3 Effected Factors Analysis

3.1 Environmental Factors

The jacking system control was impacted by seabed characteristics, environmental conditions, and the depth of the water layer. Furthermore, a variety of marine platforms are used in offshore locations for the exploration and making of energy from oil and gas. Thus, the scope of this research is restricted to areas of oceanographic ambient variables that impact the control process of JuR's jacking system. As a result, the jacking system must be capable of withstanding the following loads:

$$F_{envi} = F_{wave} + F_{wind} + F_{current} \tag{9}$$

The Wave Force. In offshore operation, the most characteristic impact is the wave. In six degrees of freedom, they attack an offshore structure to surge, sway, heave, roll, pitch and yaw. They are the primary source of workplace inefficiencies and downtime. In jacking systems, the pressures which are produced by waves play an important role in the design process. Wave factor affecting the jacking system is determined by equation [5, 7, 22, 23]:

$$F_{wave} = \xi(x, y, t) = \sum_{q=1}^{N} \sum_{r=1}^{M} \sqrt{2S(\omega_q \psi_r)\Delta\omega\Delta\psi}\, sin\left(\omega_q t + \phi_{qr} - k_q(xcos\psi_r + ysin\psi_r)\right) \tag{10}$$

where the phase angle $\phi_{qr} \in [0 - 2\pi]$, ψ_r denote direction, ω_q frequency, and S wave spectrum. The $\Delta\omega$ and $\Delta\psi$ factors represent the harmonic amplitudes of wave frequency ω_q. Besides that, $k_q = 2\pi/\lambda_q$ is the number of waves, in which λ_q is the wavelength.

The Wind Force. Wind force affects the floating stability of the truss and it depends on the windbreak area, velocity, structure shape, height. There are four methods of calculating wind load: numerical simulation, using the combined formula from experiment, field test, and wind tunnel [3, 9]. However, if the system works under the condition that the wind frequency and direction are modeled as slowly changing quantities, the wind force can be calculated by the formula [7]:

$$\begin{aligned} F_{wind} &= [X_{wind}, Y_{wind}]^T \\ X_{wind} &= 0.5 C_X g_R \rho_w V_R^2 A_T \\ Y_{wind} &= 0.5 C_Y g_R \rho_w V_R^2 A_T \end{aligned} \tag{11}$$

The wind traction into the ichnography region A_T is represented by C_X and C_Y. V_R, g_R is the speed and direction of wind acting on the truss.

The Current Force. The flow is considered to be stable even though the flow velocity varies with time, space, depth, and vortex vibration [24]. Assume that the direction and amplitude of the current are unchanged, thus correcting the current speed V_c and the direction β_c are modeled as the slow variable quantities according to the earth coordinates. Equation (12) presents the current relative speed of Jack-up coordinates [25]:

$$\begin{aligned} u_c &= V_c \cos(\beta_c - \psi_L - \psi_H) \\ v_c &= V_c \sin(\beta_c - \psi_L - \psi_H) \\ \tau_{current} &= [u_c, v_c, 0]^T \end{aligned} \tag{12}$$

where u_c and v_c represent current speed compositions, while ψ_L and ψ_H designate the angular configurations impacted by low and high-frequency values, respectively.

3.2 Internal Factors

The internal factors affect to the jacking control system, in which vibrations for the JuR's hull [3, 4, 26] are mainly caused by the periodic action of waves and currents. We have suitable methods such as dynamic factor amplification, frequency domain analysis, or time-domain analysis [27] for vibration analysis of marine structures. Using the Dynamic Amplification Factor (DAF) method [28] where the inertial load is used to represent dynamic load, the ratio between dynamic response amplification and static response amplification is calculated as follows:

$$DAF = \frac{1}{\sqrt{\left[1 - \left(\frac{T_N}{T}\right)^2\right]^2 + \left(2\varepsilon \frac{T_N}{T}\right)^2}} \tag{13}$$

with T_N is a natural period of the platform and T is a wave excitation period, and ε is the platform damp ratio taken as 0.07. Based on the weight of JuR (M > 2500 ton), the DAF coefficient is chosen to be 1.1 [29].

4 Self-adaptive Fuzzy Controller for Jacking System

4.1 Fuzzy PID Controller

To control the nonlinear model, a popular strategy combines the linear control method with the intelligent control method to promote the flexible structure and fast-response

time. Moreover, the FPID control is often chosen in the industrial application's control. In this paper, authors introduce the FPID controller as follow [30]:

$$u_{FPID}(s) = K_p(s)e(s) + K_i(s)\int_0^s e(s)ds + K_d(s)\frac{de}{ds} \tag{14}$$

The coefficients $K_p(s)$, $K_i(s)$, and $K_d(s)$ have a flexible structure according to the input variable error instead of the fixed coefficients K_p, K_i, and K_d, respectively. Thus, the normal PID controller is given by [31]:

$$u_{PID}(s) = K_p + \frac{K_i}{s} + K_d s \tag{15}$$

The flexible coefficients $K_p(s)$, $K_i(s)$, and $K_d(s)$ are updated after each control cycle according to the erroneous amplitude. Then, the PID coefficient is updated by:

$$\begin{cases} K_p(s) = K_p(s-1) + u_f(\Delta kp) \\ K_i(s) = K_i(s-1) + u_f(\Delta ki) \\ K_d(s) = K_d(s-1) + u_f(\Delta kd) \end{cases} \tag{16}$$

The updated coefficients $u_f\left(u_f(\Delta kp), u_f(\Delta ki), u_f(\Delta kd)\right)$ are defined by the fuzzy system. The notation of membership functions (MFs) for NB is Large Negative, for NBB is Near Big Negative, for NS is Small Negative, for NSS is Near Small Negative, for ZE is Zero, for PSS is Near Small Positive, for PS is Small Positive, for PBB is Near Big Positive, and for PB is Large Positive. In addition, we use a fuzzy system with a double-input $e(t)\{NB\ NBB\ NS\ NSS\ ZE\ PSS\ PS\ PBB\ PB\}$, $de/d(t)\{NB\ NS\ ZE\ PS\ PB\}$, and a triple-output $K_p\{ZE\ PSS\ PS\ PBB\ PB\}$, $K_i\{ZE\ PSS\ PS\ PBB\ PB\}$ and $K_d\{ZE\ PSS\ PS\ PBB\ PB\}$ to calibrate the coefficients $K_p(s)$, $K_i(s)$, and $K_d(s)$ [22]. Moreover, B^i, the rule designation form in Eq. (17), is a binary variable representing the rule outcome.

$$R_i : if\ \hat{e}_1\ is\ A_1^i ...and\ \hat{e}_n\ is\ A_n^i\ then\ u\ is\ B^i \tag{17}$$

for $A_1^i,\ A_2^i, \ldots A_n^i$ and B^i denote the fuzzy sets. The update coefficient can be generated by using the center average defuzzifier as follows:

$$u_f = \frac{\sum_{i=1}^{h} B^i[\prod_{j=1}^{n} \mu_{A_j^i}(\hat{e}_j)]}{\sum_{i=1}^{h}[\prod_{j=1}^{n} \mu_{A_j^i}(\hat{e}_j)]} \tag{18}$$

where $\mu_{A_j^i}(\hat{e}_j)$ express the MFs, h indicates the amount of if-then rules [9, 32]. However, the FPID algorithm controls the jacking system in time-varying environmental conditions, the results are not feasible. Therefore, we suggest the optimal solution, named fuzzy particle swarm optimization, to improve the process control quality under extreme weather conditions. Finally, the FPSO operation mechanism is introduced in the next section.

4.2 Fuzzy Particle Swarm Optimization Controller

The time-varying influences of the environmental conditions cause the jacking system's position to be inaccurate. To overcome the incorrect position, we proposed the FPSO controller with a flexible structure and optimum parameter values. As a result, the proposed solution's purpose is to adapt the control structure to react to the systematic error caused by the coefficient's environmental impact δ_λ. In addition, the PSO algorithm (λ_i) is employed to find the best parameters for enhancing response quality. Figure 3 illustrates the suggested model's mechanism, which is divided into two main stages [10]:

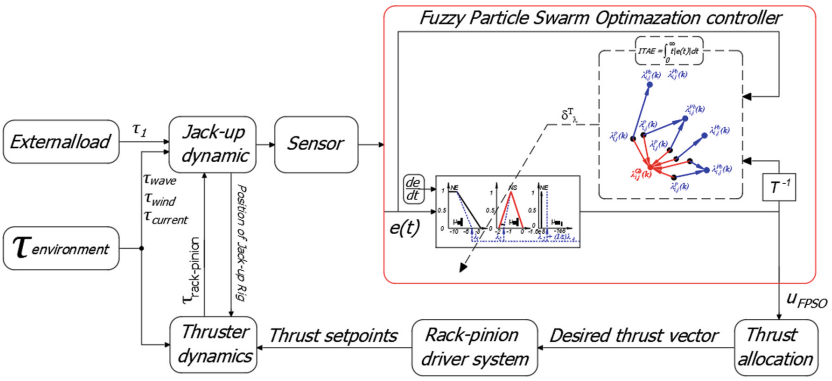

Fig. 3. The FPSO controller structure for the jacking system.

The First Stage. We establish a fuzzy structure on m.file format with the MFs flexible value to improve flexible structure. Therefore, the fuzzy modulator has a single-output $u_F(t)$ and a double-input $e(t)$, de/dt calibrating by a δ_λ coefficient to maximize the effectiveness of the fuzzy structure. The fuzzy output performance is represented as

$$u_{FPSO} = \frac{\sum_{i=1}^{h} B^i [\prod_{j=1}^{n} \mu_{A^i_{\lambda j}}(\hat{e}_j)]}{\sum_{i=1}^{h} [\prod_{j=1}^{n} \mu_{A^i_{\lambda j}}(\hat{e}_j)]} \tag{19}$$

where $\mu_{A_1^j}(\hat{e}_1) = [\lambda_1\left(A_1^1, A_1^2, \ldots A_1^j\right)]$ is the fuzzy set of the error $e(t)$, $\mu_{A_2^j}(\hat{e}_2) = [\lambda_2\left(A_2^1, A_2^2, \ldots A_2^j\right)]$ is the fuzzy set of the error-velocity de/dt, and $\delta_\lambda = \left[(\lambda_3 + \lambda_4/s)\left(B^1, B^2, \ldots B^i\right)\right]$ is the adaptive adjustable coefficient corresponding the fuzzy set of output $u_F(t)$. The fuzzy inference i is represented by the j coefficient, which is an index of the fuzzy set. Then, $\varphi_\lambda(\hat{e}) = \left[\varphi^1, \varphi^2, \ldots, \varphi^h\right] \in R^h$ expresses the fuzzy basis vector which is determined as [7]

$$\varphi_{\lambda}(\hat{e}) = \frac{[\prod_{j=1}^{n} \mu_{A_{\lambda j}^{i}}(\hat{e}_j)]}{\sum_{i=1}^{h}[\prod_{j=1}^{n} \mu_{A_{\lambda j}^{i}}(\hat{e}_j)]} \tag{20}$$

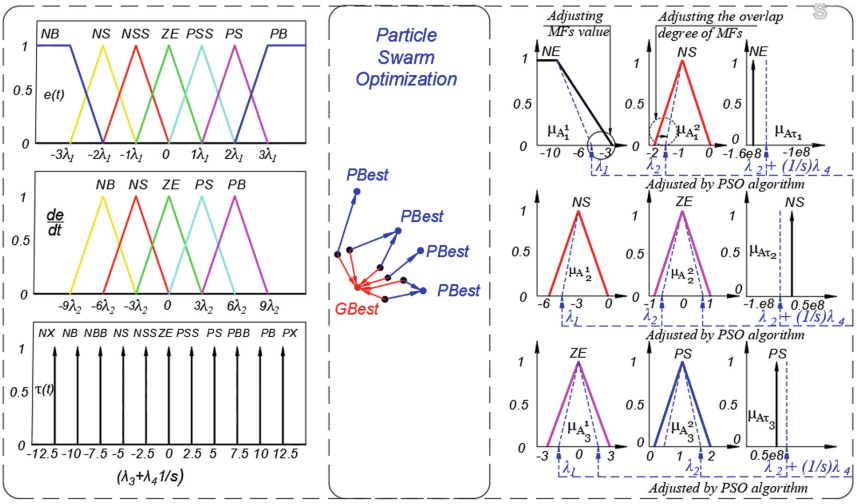

Fig. 4. The fuzzy MFs are optimally calibrated using the PSO algorithm.

The Second Stage. Aiming to determine the optimal calibration coefficient λ_i, the PSO algorithm completes the correction of fuzzy set values with coefficient $\lambda_i(\lambda_1, \lambda_2, \lambda_3, \lambda_4)$ to achieve the optimal parameters. Figure 4 represents the calibrating fuzzy MFs using the PSO algorithm. Following Eq. (20), the FPSO response can be described as

$$u_{FPSO} = \delta_{\lambda}\varphi_{\lambda}(\hat{e}) \tag{21}$$

The determination of optimal coefficient λ_i based on the PSO algorithm [10], to deal with the improving control quality in the time-varying environmental condition is represented in Algorithm 1.

Algorithm 1: The PSO algorithm calibrates the fuzzy parameter optimally [10]

Initialization:

for each particle i $(1 \le i \le s)$ **do**

Randomly initialize the position $\lambda_i^p(k)$

Randomly initialize the velocity $v_i(k)$

Initialize calibration coefficient λ_i $(\lambda_1, \lambda_2, \lambda_3, \lambda_4)$

end for

for each iteration k **do**

(a) Each particle $\lambda_i^p(k)$ update the values of $\lambda_{i,j}^p(k)$ and $\lambda_{i,j}^{Gb}(k)$

$$\lambda_{i,j}^p(k+1) = \begin{cases} \lambda_{i,j}^p(k), if\ J\left(\lambda_{i,j}^p(k+1)\right) \ge J\left(\lambda_{i,j}^p(k)\right) \\ \lambda_{i,j}^p(k+1), \qquad otherwise \end{cases} \tag{22}$$

$$\lambda_{i,j}^{Gb}(k+1) = argmin_{\lambda_{i,j}^{Pb}} J\left(\lambda_{i,j}^{Pb}(k+1)\right), 1 \le i \le s \tag{23}$$

(b) Initialize the particle attribute $v_i(k)$

$$v_{i,j}(k+1) = w(k)v_{i,j}(k) + c_1 r_1\left[\lambda_{i,j}^{Pb}(k) - \lambda_{i,j}^p(k)\right] + c_2 r_2\left[\lambda_j^{Gb}(k) - \lambda_{i,j}^p(k)\right] \tag{24}$$

where

$$w(g) = \frac{(iter_{max} - g)(w_{max} - w_{min})}{iter_{max}} + w_{min} \tag{25}$$

(c) Determine the new position $\lambda_{i,j}^p(k)$

$$\lambda_{i,j}^p(k+1) = \lambda_{i,j}^p(k) + v_{i,j}(k+1) \tag{26}$$

(d) Apply newly coefficient $\lambda_{i,j}^p(k)$ to adjust the amplitude values of the MFs and compute a fitness value according to the criteria efficiency.

$$ITAE = \int_0^\infty t|e(t)|dt \tag{27}$$

(f) A suitable point to start is to compare the obtained value to the termination condition. If the convergence criteria do not fulfill the criterion, raise k and return to step 1. (a).

end for

5 Simulation and Evaluation

5.1 Configuration Parameter

To evaluate the efficiency of the proposed method, performance comparisons between the proposed FPSO controller and the FPID controller [21] are carried out by simulation. Moreover, the parameters of the TamDao05 JuR model are used in this study. The parameter dimensions scale down by the ratio of 1:100 shown in Table 1.

Table 1. Parameters of TAMDAO05 JuR model

Description	Specifications
Type of offshore	Jack-up
Length overall	1.62 m
Breadth overall	0.96 m
Hull depth at side	0.232 m
Hull weight	0.0327 ton
Weight of a leg of the rig	0.012 ton
Number of DC motor	06
Jack-up weight	0.0928 ton
Conversion factor k_e	33.33
Torque constant K_t	1.28
Back emf constant K_b	0.0045
Armature resistance R_a	11.4
Inductance L_a	0.1214
Rotor inertia J	0.02215
Viscous friction constant D_a	0.002953

Table 2. The parameters setting of the environmental impact [9]

Description	Symbol	Specifications
Wave height	H_s	0.8 m
Wave spectrum peak frequency	ω_0	0 rad/s
Wave direction	ψ_0	30^0
Spreading factor	s	2
Number of frequencies	N	20
Number of directions	M	10
Cutoff frequency factor	ξ	3
Wave component energy limit	k	0.005
Wave direction limit	ψ_{lim}	0
Wind traction into the ichnography region	A_T	2.4
Wind speed	V_ω	2 m/s
Angle of impact wind	β_ω	20^0
Current speed	V_c	2 m/s
Jack-up direction	β_c	30^0
Low frequency and high frequency of rotation	ψ_L, ψ_H	0^0
Dominating wave frequency	w_0	0.8976 rad/s
Damping coefficient	λ	0.1
Wave intensity	σ	$\sqrt{2}$

We used the Matlab 2019a software to simulate the designed controllers under the same environmental conditions and parameters of the jacking system. Similarly, the PSO searching algorithm identifies the optimal value of the fuzzy controller to attain the best convergence on control by using the m.file interacted to Simulink. Nevertheless, these optimal coefficients support adjusting the MFs value of the fuzzy controller to fulfill the control requirement. The parameters of the environmental impact are given in Table 2 [9].

5.2 Simulation Results

We compare the achievement of the FPID and FPSO controllers in this section. The simulation schematic is shown in Fig. 5. Then, the simulation results present in Figs. 6, 7, and 8 demonstrated how the control force performs the jacking system's actual position responses (FPID in blue and FPSO in red) under the effect of environmental disturbances. In this case, the control forces acting on the legs are transformed into a certain amount of torque on the motor shaft.

The proposed FPSO controller (presented in Sect. 4.2) is carried out on the Tam-Dao05 JuR model in three case studies corresponding to levels 1, 5, and 7 of the sea state. In the simulation pocess, the FPSO controller with the optimal coefficient $\lambda_k\left(1.279 \times 10^{18},\ 1.828 \times 10^{18},\ 1.225 \times 10^{18},\ 8.743 \times 10^{17}\right)$ and the limitations of adaptive coefficient $\delta_{min}\left(-1.7053 \times 10^{17}\right) \leq \delta_\lambda \leq \delta_{max}\left(1.7053 \times 10^{17}\right)$ is used to force the jacking system to arrive at the 10 cm position in around 48 s.

5.2.1 Case Study 1

The FPID and FPSO controllers perform on the jacking system under environmental force similar to the level 1 sea state. The simulation results that apply the FPID and FPSO controllers are pointed out in Fig. 6. The simulation results showed positions of the JuR hull satisfy the overshoot, response time, and fluctuation requirements. Maximum overshoots are 2.9 cm and 0.15 cm, respectively, of the FPSO and FPID in the details. The

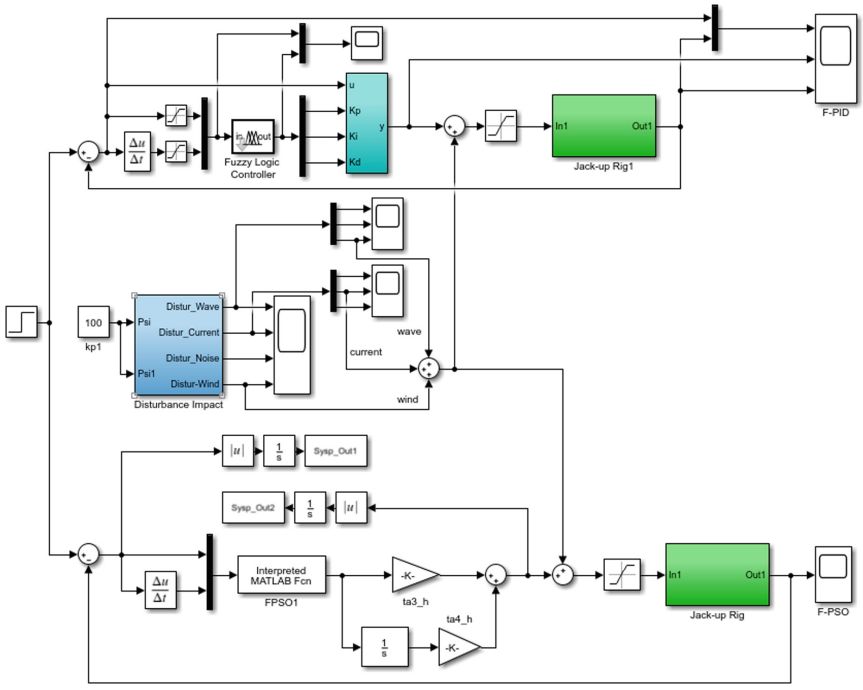

Fig. 5. The simulation schematic of the FPSO and FPID controllers for JuR model.

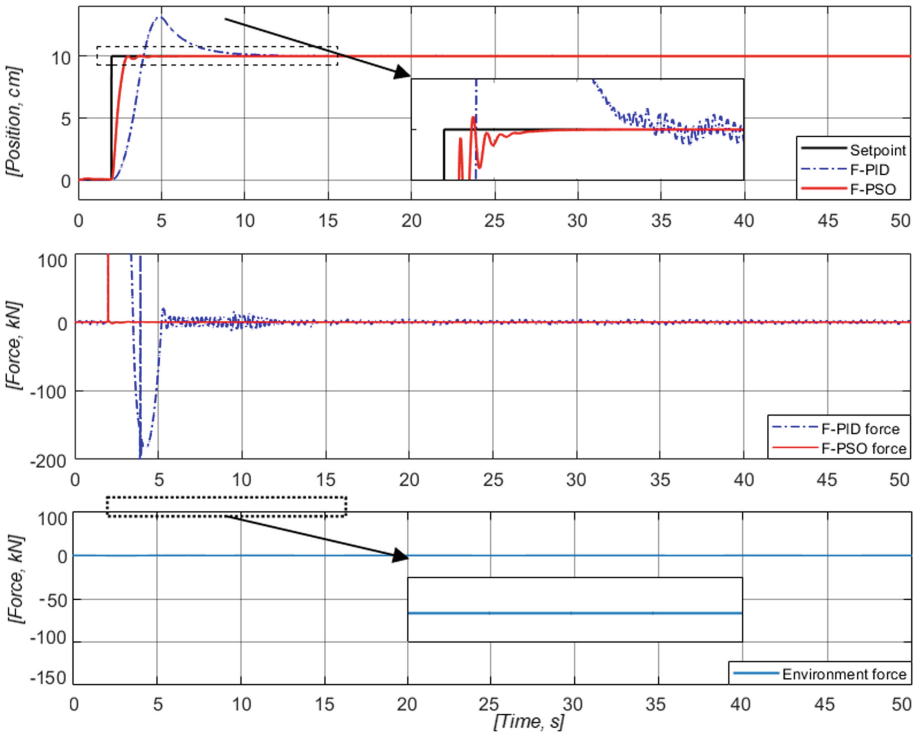

Fig. 6. The actual position, control forces, and environmental forces in the level 1 sea state.

proposed FPSO controller has a response time of around 3.5 s, which is faster than the FPID controller. Furthermore, the FPSO has a significantly smaller fluctuation amplitude than the FPID.

5.2.2 Case Study 2

In this case, the proposed solution controls the jacking system operation to reach the desired position of environmental force similar to the level 5 sea state. From the Fig. 7, the overshoot amplitude of the FPSO controller is lower than the FPID controller approximately 3.2 cm. On the other hand, the comparison results also show that the FPSO solution is satisfactory in terms of response time and fluctuation. Obviously, the FPSO solution can maintain the response quality for jacking system under changing environmental conditions.

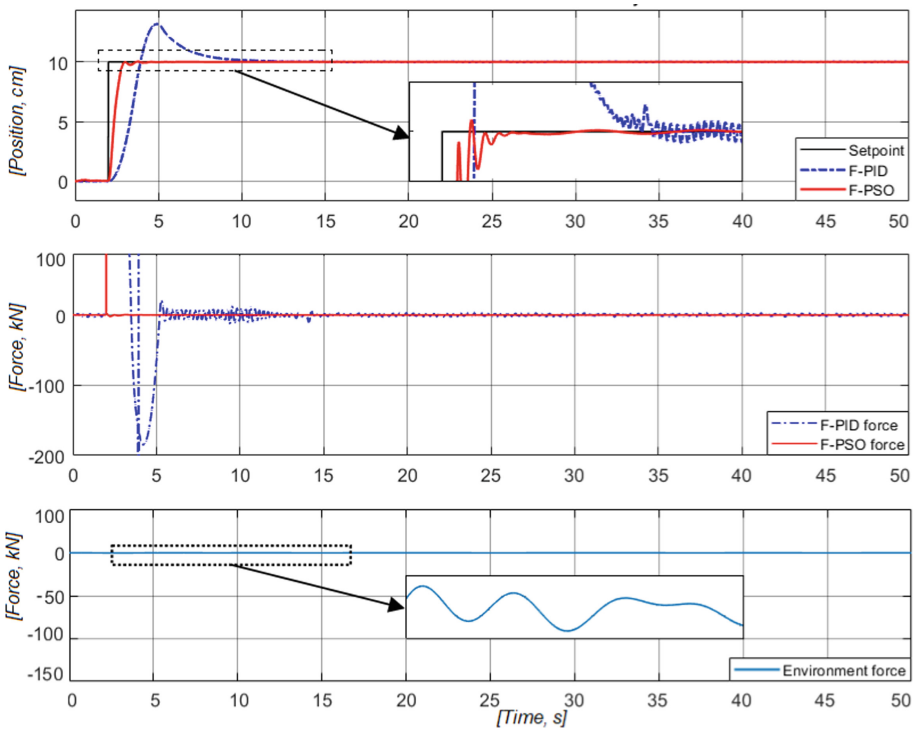

Fig. 7. The actual position, control forces, and environmental forces in the level 5 sea state.

5.2.3 Case Study 3

In this subsection, the FPSO solution are used to control stability of the JuR hull position in the extreme weather conditions (the environmental force comparable to the level 7 sea state). Figure 8 shows the fluctuation amplitude and response time when using the FPSO solution is 0.16 cm lower, 4.8 s faster, respectively, compared to the FPID controller. Futhermore, the overshoot amplitude of the proposed solution has outstanding quality over the FPID controller under the same operating conditions. The feasibility results indicate that the proposed solution is capable of adaptability disturbances caused by the environmental force.

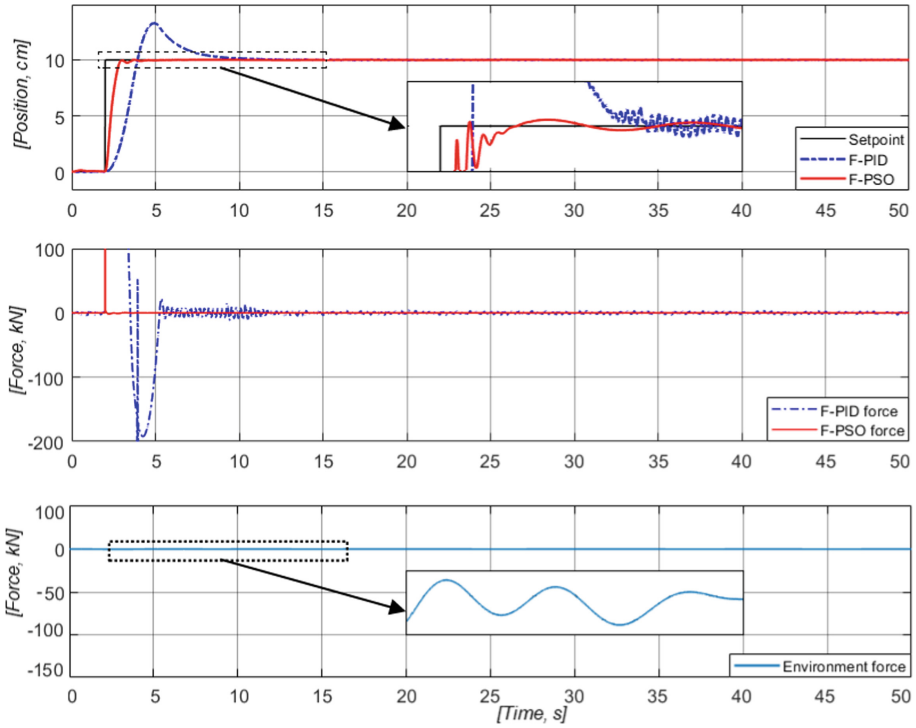

Fig. 8. The actual position, control forces, and environmental forces in the level 7 sea state.

In sum, the jacking system performance of the FPID controller is satisfactory in case 1, but unsatisfactory in cases 2 and 3, whereas the FPSO controller exhibits the similar satisfactory control performance in each case. This is because the FPID controller with control force hasn't the adaptability to the time-varying environmental forces, whereas the proposed controller has the adaptability due to exploiting the adaptive ability of δ_λ coefficient. In addition, the response of the jacking system can be enhanced by the optimal coefficient λ_k in the proposed FPSO controller. Though, the proposed solution necessitates testing in other actual working conditions to verify its advantage.

6 Conclusion

This paper has an overview of the control method for JuRs, especially in the jacking system. The movements of the JuR in the axis are analyzed and used to build the mathematical modeling of the Jacking system. Moreover, to improve the control performance of the fuzzy controller, the PSO algorithm is considered an effective solution for fuzzy self-adaptive control methods. The increase of adaptability and stability of the proposed controller for the jacking system demonstrated the effectiveness of the FPSO compared to the FPID controller in simulation. The JuR jacking control system can be enhanced performance by improving a robust algorithm in harsh conditions in the next study.

References

1. Yi, J.T., Liu, F., Zhang, T.B., Qiu, Z.Z., Zhang, X.Y.: Determination of the ultimate consolidation settlement of jack-up spudcan footings embedded in clays. Ocean Eng. **236**, 1–13 (2021)
2. Yin, Q., et al.: Field experimental investigation of punch-through for different operational conditions during the jack-up rig spudcan penetration in sand overlying clay. J. Petrol. Sci. Eng. **195**, 1–21 (2020)
3. Wang, F., Xiao, W., Yao, Y., Liu, Q., Li, C.: An analytical procedure to predict transverse vibration response of Jack-Up Riser under the random wave load. Shock. Vib. **2020**, 1–9 (2020)
4. Xie, Y., Huang, J., Li, X., Tian, X., Liu, G., Leng, D.: Experimental study on hydrodynamic characteristics of three truss-type legs of jack-up offshore platform. Ocean Eng. **234**, 1–15 (2021)
5. Dang, X.K., Ho, L.A.H., Do, V.D.: Analyzing the sea weather effects to the ship maneuvering in Vietnam's Sea from Binh Thuan Province to Ca Mau Province based on fuzzy control method. TELKOMNIKA (Telecommun. Comput. Electron. Control) **16**(2), 533–543 (2018)
6. Pashna, M., Yusof, R., Ismail, Z.H., Namerikawa, T., Yazdani, S.: Autonomous multi-robot tracking system for oil spills on sea surface based on hybrid fuzzy distribution and potential field approach. Ocean Eng. **207**, 1–11 (2020)
7. Dang, X.K., Do, V.D., Nguyen, X.P.: Robust adaptive fuzzy control using genetic algorithm for dynamic positioning system. IEEE Access **8**, 222077–222092 (2020)
8. Wang, S., Yin, X., Li, P., Zhang, Y., Wang, X., Tong, S.: Cognitive control using adaptive RBF neural networks and reinforcement learning for networked control system subject to time-varying delay and packet losses. Arab. J. Sci. Eng. **46**(10), 10245–10259 (2021). https://doi.org/10.1007/s13369-021-05752-y
9. Do, V.-D., Dang, X.-K., Huynh, L.-T., Ho, V.-C.: Optimized multi-cascade fuzzy model for ship dynamic positioning system based on genetic algorithm. In: Duong, T.Q., Vo, N.-S., Nguyen, L.K., Vien, Q.-T., Nguyen, V.-D. (eds.) INISCOM 2019. LNICSSITE, vol. 293, pp. 165–180. Springer, Cham (2019). https://doi.org/10.1007/978-3-030-30149-1_14
10. Do, V.-D., Dang, X.-K.: The fuzzy particle swarm optimization algorithm design for dynamic positioning system under unexpected impacts. J. Mechan. Eng. Sci. **13**(3), 5407–5423 (2019)
11. Dang, X.-K., Do, V.-D., Do, V.-T., Ho, L.-H.: Enhancing the control performance of automatic voltage regulator for marine synchronous generator by using interactive adaptive fuzzy algorithm. In: Vo, N.-S., Hoang, V.-P., Vien, Q.-T. (eds.) INISCOM 2021. LNICSSITE, vol. 379, pp. 379–392. Springer, Cham (2021). https://doi.org/10.1007/978-3-030-77424-0_31
12. Fateh, S., Fateh, M.M.: Adaptive fuzzy control of robot manipulators with asymptotic tracking performance. J. Control Autom. Electr. Syst. **31**(1), 52–61 (2019). https://doi.org/10.1007/s40313-019-00496-5
13. Xiaowei, G., Shen, Q.: A self-adaptive fuzzy learning system for streaming data prediction. Inf. Sci. **579**, 623–647 (2021)
14. Buzura, S., Dadarlat, V., Iancu, B., Peculea, A., Cebuc, E., Kovacs, R.: Self-adaptive fuzzy QoS algorithm for a distributed control plane with application in SDWSN. In: 2020 IEEE International Conference on Automation, Quality and Testing, Robotics (AQTR), pp. 1–6 (2020)
15. Thomas, V.K.S., Ashok, S.: Fuzzy controller-based self-adaptive virtual synchronous machine for microgrid application. IEEE Trans. Energy Conv. **36**(3), 2427–2437 (2021)
16. Dang, X.-K., Tran, T.-D.: Modeling techniques and control strategies for jack-up rig: a state of the art and challenges. IEEE Access **9**, 155763–155787 (2021)

17. Dokainish, M.A., Subbaraj, K.: A survey of direct time-integration methods in computational structural dynamics—I explicit methods. Comput. Struct. **32**(6), 1371–1386 (1989)
18. Veletsos, A.S., Ventura, C.E.: Modal analysis of non-classically damped linear systems. Earthq. Eng. Struct. Dynam. **14**, 217–243 (1986)
19. Jong-Shyong, W., Chang, C.-Y.: Structural simplification of jackup rig and its dynamic responses in regular waves. J. Ship Res. **32**(2), 134–153 (1988)
20. Ben, C.: Gerwick: Construction of Marine & Offshore Structures. 3rd edn. Taylor & Francis Group, LLC (2007)
21. Do, V.D., Dang, X.K., Le, A.T.: Fuzzy adaptive interactive algorithm for rig balancing optimization. In: International Conference on Recent Advances in Signal Processing, Telecommunication and Computing, Danang, Vietnam, pp. 143–148 (2017)
22. Dang, X.-K.: Le Anh-Hoang Ho: Joint fuzzy controller and fuzzy disturbance compensator in ship autopilot system: investigate stability in environmental conditions. J. Curr. Sci.Technol. **11**, 114–126 (2021)
23. Fossen, T.I.: A survey on nonlinear ship control: from theory to practice. IFAC Conf. Manoeu. Control Marine Craft **33**(21), 1–16 (2000)
24. American Bureau of Shipping: ABS Rules For Building and Classing Mobile Offshore Drilling Units. American Bureau of Shipping, New York (2014)
25. Fossen, T.I.: Handbook of Marine Craft Hydrodynamics and Motion Control. John Wiley & Sons, Ltd., Chichester (2011)
26. Abdulrahman, M.: Reyad: environmental load effects at offhore Jack-up unit. Int. J. Sci. Eng. Res. **9**(10), 1349–1369 (2018)
27. Zhen, W., Zhigao, Z.: Damage detection of offshore platform structures using time domain response Data. In: IEEE/International Conference on Intelligent Computation Technology and Automation, pp. 1079–1084 (2010)
28. Society of Naval Architects and Marine Engineers: SNAME Technical and Research Bulletin 5–5A Site Specific Assessment of Jack-up Units. Society of Naval Ar-chitects and Marine Engineers, New Jersey (2012)
29. Subrata, K.: Chakrabarti: Handbook of Offshore Engineering-Offshore Structure Analysis, 1st edn. Plainfield, Illinois (2005)
30. Dang, X.K., Guan, Z.H., Li, T., Zhang, D.X.: Joint Smith predictor and neural network estimation scheme for compensating randomly varying time-delay in networked control system. In: Proceedings of the 24th Chinese Control and Decision Conference, Tai Yuan, China, pp. 512–517 (2012)
31. Salih, A.M., Humod, A.Th., Hasan, F.A.: Optimum design for PID-ANN controller for automatic voltage regulator of synchronous generator. In: Proceedings of 4th Scientific International Conference Najaf (SICN), Al-Najef, Iraq, pp. 74–79 (2016)
32. Sharma, R., Gopal, M.: A Markov game-adaptive fuzzy controller for robot manipulators. IEEE Trans. Fuzzy Syst. **16**(1), 171–186 (2008)